

Infiltration Investigation of a Radiantly Heated and Cooled Office

Xiangyang Gong David E. Claridge Phd P.E
Graduate Student Professor
Energy Systems Laboratory
Department of Mechanical Engineering
Texas A&M University

David H. Archer PhD
Professor
Center for Building Performance and Diagnostics
School of Architecture
Carnegie Mellon University

ABSTRACT

Air infiltration has a significant impact on the heating and cooling loads of small office and residential buildings. In a radiantly heated and cooled office, air infiltration normally determines whether this type of system can operate without condensation on the radiant cooling surface in summer, because infiltration may bring considerable moisture into the space. The office studied experiences infiltration that seriously limits the effectiveness of the radiant cooling system and active desiccant dehumidification system. Earlier infiltration measurements using the tracer gas procedure showed infiltration levels of 0.78 – 1.12 ACH, while CO₂ concentration measurements gave values from 0.1 – 0.2 ACH. This paper reports the results of infiltration levels determined from blower door measurements and logged humidity data from the ventilation unit as well as a reanalysis of the CO₂ data. There were still significant discrepancies that are resolved by combining the measured results with a calibrated simulation and additional site measurements. It is found that infiltration in the studied office is from two sources: one is outdoor air; the other is the indoor air from the floor below the studied office. The total air infiltration for the studied space may vary from 0.74ACH in the summer to 1.5ACH in the winter, while the under floor space air leaking into the studied office may range from 0.46-1.03ACH.

INTRODUCTION

To provide a comfortable and healthy indoor environment for building occupants, an adequate outside air supply is necessary to dilute and remove indoor air contaminants. Outside air is normally provided by mechanical ventilation in commercial buildings and by natural ventilation in residential buildings. However, the energy required to condition the outdoor air is often a significant portion of the total space conditioning load. Large commercial buildings normally operate continuously at a slightly pressurized condition in which air infiltration is expected to have less impact on building conditioning load. In small office buildings and residential buildings, the air infiltration often has a significant impact on the space conditioning load since the buildings are not pressurized and air conditioning

systems operate intermittently. In a radiantly heated and cooled office, the infiltration not only has an impact on building heating and cooling load; it also strongly affects the indoor humidity level and hence the ability to operate the radiant cooling panels without condensation. The magnitude of the infiltration into this type of the building must be known in order to size the radiant panels and dehumidification equipment for this type of system properly.

Significant research has been done on building air flow models and infiltration measurement procedures. Building air flow models can be classified as single zone models and multizone models. A widely used multizone model is COMIS which was developed by Feustel and Raynor-Hoosen [1], and improved by Feustel [2]. The single zone model LBNL model developed by Sherman and Grimsrud [3] has been used very widely. Walker and Wilson [4] also proposed a well recognized enhanced single zone model. For small office buildings and residential buildings, the single zone model is applicable. According to Persily [5] and Walker and Wilson [6], these models can have an error of 40% or higher. In order to obtain an applicable yearly infiltration profile, these models should be combined with air infiltration measurements. Commonly used infiltration measurement procedures include the tracer gas method, CO₂ concentration decay method, blower door test method, etc.

The office studied in this paper is a small university office area which includes space for faculty, graduate student and staff offices and a meeting room at a university in Pittsburgh, PA. This office space, with an area of 580 m² (6228 ft²), uses a radiant heating and cooling system combined with a solid desiccant ventilation unit. Gong and Claridge [7] studied the indoor humidity levels of this radiantly heated and cooled space and noted that infiltration was the main factor which affecting operation of the cooling system without condensation on the panels and energy efficiency of the radiant system. In order to accurately simulate the heating and cooling consumption of the space and precisely size the equipment in the energy supply and energy distribution systems, the infiltration level of the space needs to be carefully measured and studied. This

paper provides an overview of previous infiltration studies of the space, analyzes blower door measurement results and evaluates the infiltration by the LBNL model. This paper also compares infiltration measurements in the space by the tracer gas method, CO₂ concentration method, blower door test method, and logged humidity data. It then combines the differing measured results with simulation to investigate reasons for these differences and reach a conclusion on the “real” infiltration value in this office. Some possible leakage points are also identified from site measurements.

PREVIOUS INFILTRATION STUDIES OF THE SPACE

Infiltration Measurement by Tracer Gas Method

Several studies have been done to estimate the infiltration level of the space. Mahdavi et al. [8] measured the infiltration in the space using the tracer gas method. They installed six sampling points, A1-A6, as shown in Figure 1, in the space during the test conducted on March 28, 1998. They observed the average infiltration to be 0.86ACH. They performed the measurement again on April 2, 1998 using four samplers (B1, B2, B4, B6) and observed an average infiltration of 0.95ACH.

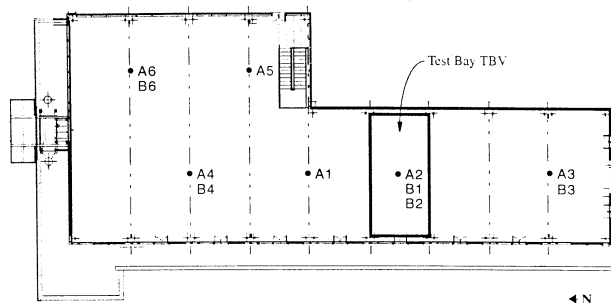


Figure 1. Tracer Gas Sampler Locations in the space During the Infiltration Measurements (Mahdavi et al. 2000)

Boonyakiat [9] also conducted a series of infiltration measurements in one bay (Bay 1) of the space in July and August of 1999. The results he obtained are listed in Table 1. Experiments numbered 2, 5, 11, and 12 in Table 1 were performed, when windows and ventilators were fully closed.

Table 1. . Infiltration of Bay 1 Using Tracer Gas Measurements (Boonyakiat, 2003)

Experiment 2	Experiment 5	Experiment 11	Experiment 12
1.12	1.31	0.82	0.78

Infiltration Measurement by CO₂ Concentration Method

Betz et al. [10] carried out a CO₂, occupancy and ventilation study in the spring of 2006. They monitored the CO₂ concentration and the number of occupants in the space during meetings on March 21 and 22, 2006, and during May, 2006. Their results calculated from the the measured CO₂ concentration values showed the infiltration to be 0.1-0.2 ACH, which seems inconsistent with the previous measured results. Their CO₂ concentration data are re-analyzed in the following section.

ANALYSIS OF CO₂ CONCENTRATION MEASUREMENT DATA

This section re-analyzes the CO₂ concentration data obtained by Betz et al. [10]. The indoor CO₂ concentration, in PPM, can be obtained as

$$C_r = C_o + \frac{\dot{V}_{gen}}{\alpha * V_r * \rho * 10^{-6}} + \left(C_{ro} - C_o - \frac{\dot{V}_{gen}}{\alpha * V_r * \rho * 10^{-6}} \right) e^{-\alpha t} \quad (1)$$

C_r in the above equation is the CO₂ level in the space. The nomenclature for the other terms and the derivation of Equation (1) are given in Appendix I.

The indoor CO₂ level and occupancy were logged every 10 minutes by three CO₂ sensors. The CO₂ concentration in the space was considered to be the average of CO₂ readings in the space. For every set of two successive measurements, the first measurement can be considered to be the initial CO₂ level, C_{ro} , and the second measurement can be considered to be the current indoor CO₂ level, C_r . If C_{ro} and C_r are known in Equation (1), the infiltration value, α , can be determined from a trial and error solution of Equation (1).

When CO₂ concentration data were logged on March 21-23, 2006, no outside CO₂ data were recorded. On May 3, the outdoor CO₂ level was logged when the second measurements were taken. The night-time outdoor CO₂ level on May 3 ranged from 345ppm to 405ppm, and significant portion of the measured data are in the range of 380ppm to 400ppm. These values are consistent with the current worldwide average CO₂ concentration of 387 PPM [11], so 387 ppm is used as the outside CO₂ concentration level in this analysis. The corresponding 10 minute ACH values calculated for March 21st and March 22nd are plotted in Figure 2. The average hourly ACH values are listed in Table 2.

From Figure 2, it can be seen that the infiltration based on this CO₂ analysis ranges widely from 0.1 to 0.9 ACH. This may be caused by CO₂ sensor error and frequent changes in the number of occupants.

The outdoor CO₂ concentration is assumed to remain constant during the analysis, since real time measurements were not available. In reality, the outdoor CO₂ concentration probably varied over time as well, which would also contribute to the scatter in apparent infiltration values. It is known that infiltration is a function of wind speed and temperature difference. The infiltration should be lower at noon and higher during the morning and evening. This tendency can be seen from the data collected on March 22, 2006, and shown in Figure 2.

To eliminate the disturbance of frequent changes in occupancy and the variation of the outside CO₂ concentration, another set of CO₂ data was taken on the night of May 3, 2006. The outdoor CO₂ concentrations were also recorded. 3-6 people stayed inside the space during that night. Figure 3 shows the inside and outside CO₂ concentration levels.

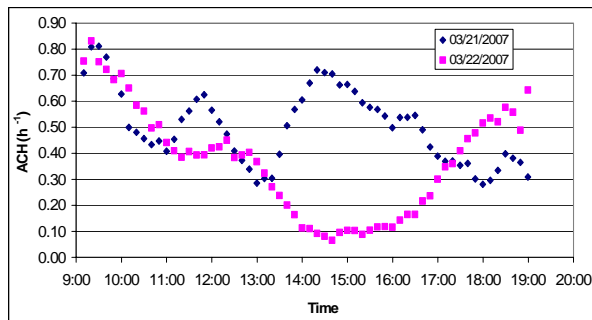


Figure 2 Air Change Rate During the Meeting on March 21 and 22, 2006

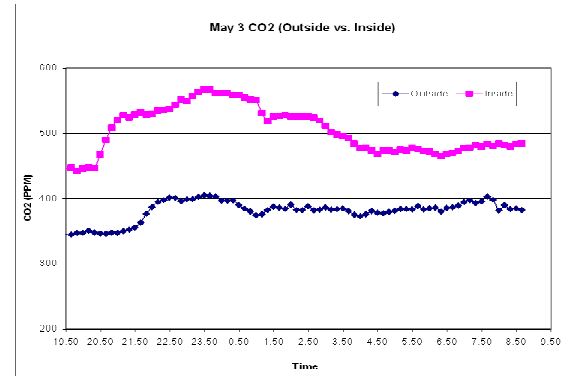


Figure 3 Indoor and Outdoor CO₂ Concentrations on the Night of May 3, 2006

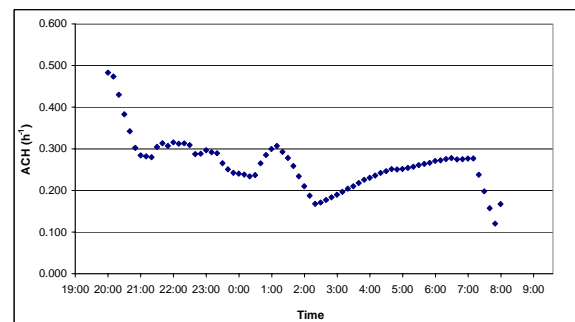


Figure 4 Overnight ACH based on CO₂ measurements of May 3-4, 2006

Table 2. Calculated Hourly Average Infiltration Rates During the Meeting on March. 21-22, 2006

Time	9:00	10:00	11:00	12:00	1:00	2:00	3:00	4:00	5:00	6:00
3/21/2006 Occupants	37	38	20	35	20	34	36	30	11	5
3/21/2006 Infiltration, ACH	0.63	0.89	0.26	0.74	0.25	0.42	0.83	0.53	0.51	0.28
3/22/2006 Occupants	35	32	27	21	18	5	5	5	8	5
3/22/2006 Infiltration, ACH	0.58	0.83	0.46	0.26	0.51	0.11	0.09	0.09	0.13	0.5

Table 3 Relative Infiltration Errors Induced by CO₂ measurement

dC_r (PPM)	5	10	15	20	25	30	35	40	45	50
$d\alpha / \alpha$	0.104	0.207	0.311	0.414	0.518	0.621	0.725	0.829	0.932	1.036

The infiltration level at each data point can be calculated using Equation (1). The nighttime infiltration levels for this set of data are plotted in Figure 4. It can be seen that the variation of

infiltration rate is much smaller than that shown in Figure 2. The nighttime ACH varies from 0.1 to 0.5.

The above analysis shows the air change rate between the indoor air and outdoor air ranges

between 0.1 and 0.9, based on the CO₂ concentration measurements.

The error analysis has been done regarding the infiltration errors induced by CO₂ concentration measurement. By assuming initial indoor CO₂ level of 420 PPM, 20 people in the office, measurement time step is 10 minutes and real infiltration is close to 0.6, the infiltration errors induced by the CO₂ measurement errors are listed in Table 3.

From Table 3, it can be found that if the error of indoor CO₂ measurement is 5PPM, the relative errors of calculated infiltration is 10.4%. If the error of the indoor CO₂ measurement is 50PPM, the relative error of calculated infiltration is 103.6%. It can be seen that the calculated infiltration rate is very sensitive the error of CO₂ measurement.

ANALYSIS OF BLOWER DOOR MEASUREMENT DATA

The blower door is a powerful diagnostic tool for measuring the infiltration of small buildings and for helping to locate air leakage points. The infiltration rates obtained from the blower door tests normally are expressed in terms of ACH50, which is the hourly air change rate at 50 Pa of fan pressure. This value can be converted into a simple estimation of the seasonal natural air change rate (ACH) by the following relation, according to Sherman and Dickerhoff [12]:

$$ACH \approx \frac{ACH_{50}}{20} \quad (2)$$

The blower door test can be a pressurization test or a depressurization test in which the blower increases or decreases the pressure within a building above or below the outdoor pressure. The depressurization test is often used in small buildings to identify the leakage sources.

Two blower door measurements were performed on the space. The first was Oct 6, 2006, and the second was on Oct 10, 2006. The measurement

results are listed in Table 4. Because the blower door is designed for use in buildings with a floor area less than 3000 ft² (279 m²) and the area of the space being tested is approximately 6200 ft² (576 m²) (the blower door fan could not produce a 50 Pa fan pressure difference during these two tests, even though the blower door cover ring was left wide open. Therefore, Equation (2) cannot be used to estimate the natural infiltration based on the measured data. The natural infiltration can be calculated by using the equivalent leakage area method (Equation 3) according to the ASHRAE Handbook [13]. When the equivalent leakage area is known, the infiltration is a function of the temperature difference and wind speed, and can be expressed by Equation (3).

$$A_L = C_s Q_r \frac{\sqrt{\rho/2\Delta P_r}}{C_D} \quad (3)$$

$$Q = A_L \sqrt{C_s \Delta t + C_w U^2} \quad (4)$$

$$\alpha = \frac{Q}{V_r} \quad (5)$$

The symbols and the values of the constant can be found in the nomenclature section.

Based on the blower door measured data, the equivalent leakage areas from these two tests are calculated and shown in Table 5. The equivalent leakage area of 1680 in² is used in the analysis in this paper, because the variation of wind velocity in the second measurement is larger and there was frequent change of occupant on the second measurement day. From the Pittsburgh TMY2 weather data file, the hourly temperature and wind speed are both given for a “typical” year. Therefore, the hourly infiltration can be calculated by Equation (4), once the equivalent leakage area A_L is known. The hourly and average daily ACH for a TMY weather year are plotted in Figures 5 and 6.

Table 4. Blower Door Measurement Results

Oct 6, 2006, Test Data	Pressure (Pa)	10.2	11.2	8.6	9	8.8
	Flow Rate (CFM)	5950	5925	5952	5935	5963
	Baseline (Pa) 0.94	Wind speed 6 mph		Temperature 38°F		
Oct 10, 2006, Test Data	Pressure (Pa)	8.6	8.2	9.1	8.4	8.6
	Flow Rate (CFM)	6026	6010	5922	6012	5992
	Baseline (Pa) 0.46	Wind speed 7 mph		Temperature 63°F		

Table 5. Equivalent Leakage Areas

	CFM	C ₅	Cd	DP(Pa)	Dp(in WG)	rho	A _L (in2)	A _L (ft2)
6-Oct-06	5945	0.186	0.65	9.56	0.0384312	0.075	1680.4	11.67
10-Oct-06	5990	0.186	0.65	8.72	0.03504234	0.075	1773.2	12.31

Table 6. Monthly Average Air Change Rates for the Space for a TMY Year Determined from the Effective Leakage Area.

Month	Temp(F)	Humidity	Wind (mph)	Indoor Temp(°F)	Temp Diff (°F)	AL(in2)	Q(CFM)	ACH
Jan	26.2	0.0021	9.6	72	45.8	1680	2137	1.49
Feb	27.6	0.0022	8.7	72	44.4	1680	2009	1.40
Mar	43.1	0.0038	8.8	72	28.9	1680	1852	1.29
Apr	47.6	0.0043	7.7	72	24.4	1680	1650	1.15
May	60.8	0.0076	6.9	72	11.2	1680	1353	0.94
Jun	69.7	0.0105	6.7	72	2.3	1680	1173	0.82
Jul	70.7	0.011	6.2	72	1.3	1680	1073	0.75
Aug	71.3	0.012	6.2	72	0.7	1680	1061	0.74
Sep	63.5	0.0096	5.4	72	8.5	1680	1091	0.76
Oct	51.7	0.006	7	72	20.3	1680	1502	1.05
Nov	41.5	0.0042	9.2	72	30.5	1680	1925	1.34
Dec	33.5	0.0031	8.7	72	38.5	1680	1946	1.36

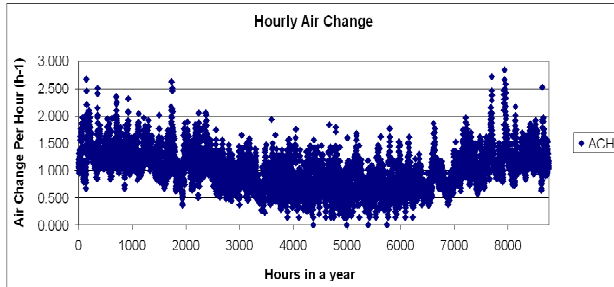


Figure 5. Hourly Infiltration in the Space for a TMY Weather Year Based on Effective Leakage Area

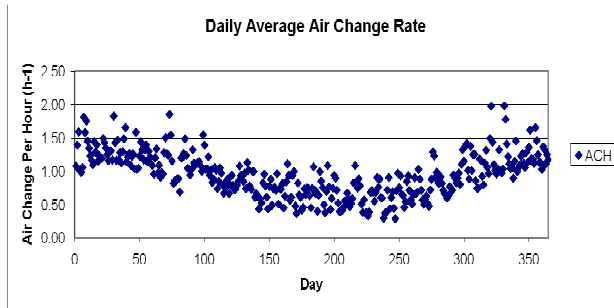


Figure 6. Average Daily Infiltration in the Space for a TMY Weather Year Based on Effective Leakage Area

From Figures 5 and 6, it can be seen that the infiltration rate is between 0.5 and 1.5ACH for most

of a typical year. The air exchange rate is higher in the winter and lower in the summer. The average monthly infiltration rates are listed in Table 6. From Table 6, we can see that the monthly average air change rate varies from 0.74 in the summer to 1.49 in the winter which is, in general, consistent with the tracer gas measurement results.

ANALYSIS OF LOGGED HUMIDITY DATA

The new control system logs the operational status of the active desiccant ventilation unit in the space beginning in 2006. The recorded values of supply air humidity ratio, indoor humidity ratio and outdoor humidity ratio provide an alternative approach to estimating the infiltration of the studied space. The moisture balance of the space can be written as:

$$\dot{W}_{in}^{\xi} - \dot{W}_{out}^{\xi} + \dot{W}_{gen}^{\xi} = \dot{W}_{storage}^{\xi} \quad (6)$$

$$\dot{W}_{in}^{\xi} = 60 * \rho * \dot{V}_s^{\xi} * w_s + \alpha * \rho * V_r * w_o \quad (7)$$

$$\dot{W}_{out}^{\xi} = 60 * \rho * \dot{V}_L^{\xi} * w_r + \alpha * \rho * V_r * w_r \quad (8)$$

By substituting Equations (6) and (7) into Equation (8) and considering $\dot{W}_{storage}^{\xi} = 0$, the following infiltration equation can be obtained:

$$\alpha = \frac{60 * \dot{V}_s^{\xi} * w_s - 60 * \dot{V}_L^{\xi} * w_r + \dot{W}_{gen}^{\xi} / \rho}{V_r * w_r - V_r * w_o} \quad (9)$$

In the above equation, \dot{V}_s^{ξ} , \dot{V}_L^{ξ} , w_s , w_r and w_o can be obtained from the control system. V_r is

known. Therefore, the infiltration can be calculated based on the logged ventilation unit operational data. One week of data (August 6-12, 2006) was taken from the control system in the summer of 2006. The supply air flow rate and humidity ratios for the period of August 6, 2006, to August 8, 2006, are plotted in Figures 7 and 8. Leaving DX AH is the absolute humidity ratio of the air leaving the DX coil. Supply AH is the absolute humidity ratio of the supply air to the space. From this measured information, the air change rate can be calculated for every 15 minute period. The results are shown in Figure 9.

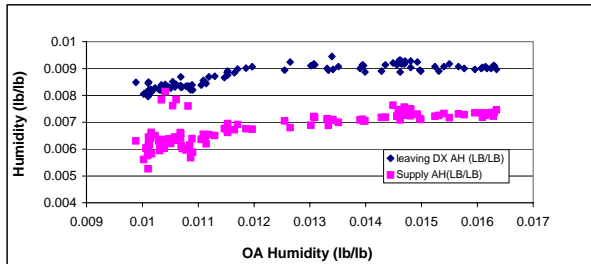


Figure 7. Supply Air Humidity Ratios

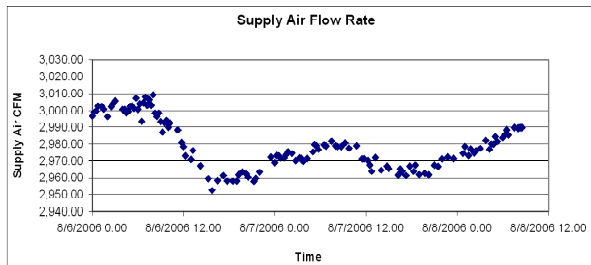


Figure 8. Supply Air Flow Rate August 6-8, 2006 (CFM)

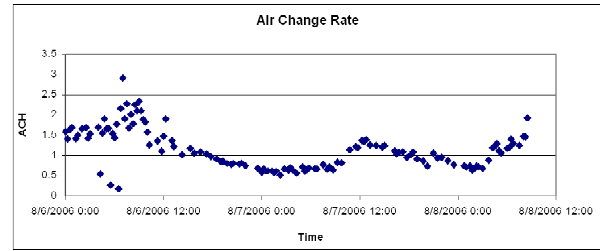


Figure 9. Air Change Rate Determined from Humidity Data

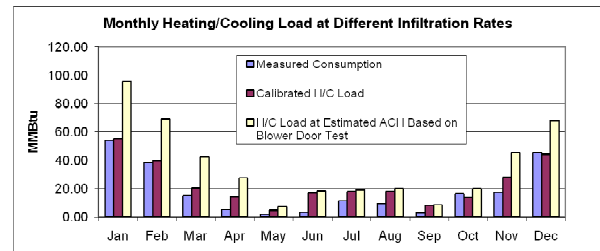


Figure 10. Monthly Heating/Cooling Loads at Calibrated and Effective Leakage Area Predicted Infiltration Rates

Table 7 Infiltration Analysis Results

Approach	Tracer Gas	CO ₂ Concentration	Blower Door Measurement	Humidity Data Analysis
Infiltration Range	0.86-0.95	0.1-0.9	0.4-2.0	0.5-2.5
Applicable Dates	July, August	March	Year round	August

From Figure 9, it can be seen that the infiltration rate varies from 0.5 to 2.5ACH during this two and a half day period, and most of the values are between 0.5 and 1.5ACH, which is larger than the summer values predicted by the blower door or the CO₂ measurement methods. These results will be discussed in the following section.

DISCUSSION

Infiltration Rate Determined by Four Different Approaches

The space infiltration rate has been determined using four different approaches in the previous

sections. These approaches are the tracer gas method, the CO₂ concentration method, the blower door measurement method and the humidity data analysis method. Table 7 shows the space infiltration ranges obtained from the four methods and their corresponding dates.

Because infiltration is a function of the indoor and outdoor temperature difference and the wind speed, it varies from month to month. The infiltration measured in different months could have different values. In summer, the blower door measurement results (Table 6) are nearly consistent with the tracer gas measurement results, the CO₂ concentration

results, and the humidity data analysis results. The summer infiltration rate for these three methods ranges from 0.5 to 0.9. Table 7 shows that the infiltration rate range from the humidity data analysis is larger than those obtained from the CO₂ concentration measurements and the blower door tests. This is thought to be due to the windows and doors being open at least part of the time when the desiccant ventilation unit is running. All spaces adjacent to the studied office are unconditioned space during the summer. Hence additional moisture can be brought into the space when the doors and windows are open. Therefore, the calculated infiltration rates based on logged humidity dates would be higher than the actual rates of infiltration from the outdoors. The CO₂ concentration method gave a relatively smaller infiltration rate than the other methods. This may be explained conceptually since some air enters the space from the third floor below the studied space, and this air will have a higher CO₂ level than outside air¹.

Air Leakage from the Third Floor

During the blower door measurements, a significant amount of air was found to blow into the space from the plenum below the space. By checking the plenum and the third floor ceiling below the plenum, it was found this air came from the third floor. Therefore, air leakage in the space can be divided into two parts: internal leakage from the third floor and external leakage from outside air. In the winter, the conditioned third floor air leaking into the studied office will not affect the heating load since there is no significant temperature difference between the studied office and the third floor in winter. In the summer, the third floor is not cooled and the stack effect drives the hot third floor air into the space. The cooling load will then be larger than that considering only the thermal envelope air leakage. Because infiltration air from outside accounts for a significant part of the building heating and cooling load, a calibrated simulation of the space should give some indication of the amount of outside air infiltration.

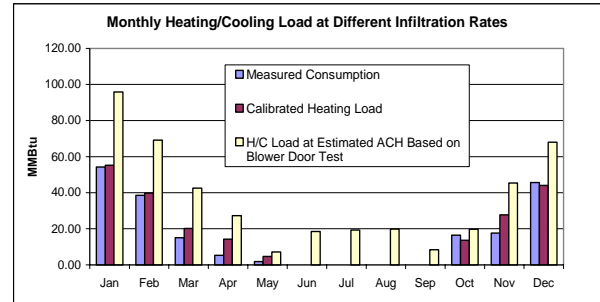


Figure 10. Monthly Heating/Cooling Loads at Calibrated and Effective Leakage Area Predicted Infiltration Rates

The space was simulated using DOE2.1 software by Gong and Claridge [7]. The simulation was carefully calibrated according to the procedure of Claridge et al [14]. Because measured cooling data for the space are not available, the calibrated simulation is based on the eight months of measured 2003 heating consumption data. The infiltration rates are carefully adjusted to ensure the simulated consumption to match up the measured consumption.

The infiltration rates used in the calibrated DOE-2.1 simulation will now be used to help explain the discrepancy between the humidity-based infiltration measurements and the other three infiltration measurements. The effective leakage area (ELA) infiltration rate will be used as a surrogate for the CO₂-based and tracer gas based infiltration measurements as well in the discussion that follows. The heating loads at the infiltration rates used in the calibrated simulation (CS infiltration) and those based on measured ELA are listed in Table 8. Figure 10 compares the monthly measured heating loads with those of the calibrated simulation and those estimated using ELA infiltration. From Figure 10, it can be seen that the heating loads at the ELA infiltration rates are much larger than the measured heating loads if all the infiltration air is assumed to be outside air. The simulation results suggest that a significant part of the infiltration air does not affect the heating load of the space. The difference between the infiltration predicted by the measured ELA and the CS infiltration rate does not affect the heating load. This part of the infiltration can be considered to be conditioned air leaking from the third floor into the space. Therefore, it is believed that the winter CS infiltration rates are actually outside air exchange rates recorded during this period. The air exchange with the third floor varies from 0.46 to 1.09ACH during the year, based on the results shown in Table 8.

¹ The CO₂ level may also be affected by CO₂ emitted or absorbed by the indoor plants, but this has not been quantified and the effect of the plants on the indoor CO₂ level is not clear at this time.

Possible Leakage Sites

The space façade is a high quality product. The windows, doors, and roofs are all tight. However, several possible leakage sites in the space envelope were identified by a site visit. The first is the joints between the metal roof and the walls. The seals at these joints are not tight. The second is the roof ventilators, as shown in Figure 11. The roof ventilators were directly open to the outside to balance the pressure difference at one time. Now the ventilators are permanently closed. However, there is a small gap between the ventilator damper and the damper frame on every ventilator. In addition, some louvers behind the ventilator damper are not closed.

A significant amount of leaking air was observed coming into space from the under floor plenum. Gaps were found around some of the ducts and pipes which penetrate the third floor ceiling. When the plenum air leaks into the space, the third floor conditioned air

leaks into the plenum through these gaps. Figure 12 shows an example of such gaps.

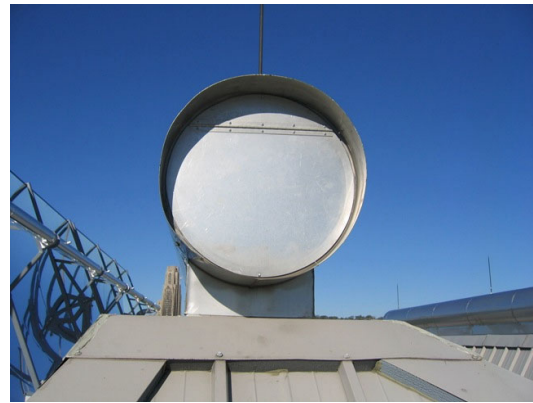


Figure 11. Potential Leakage Sites–Roof Ventilators

Table 8. Simulated heating and cooling loads at CS and ELA infiltration rates

Month	Measured Consumption (MMBtu)	CS Air Change Rates (hr ⁻¹)	Simulated Monthly Heating and Cooling Load at CS Air Change Rates	ELA Air Change Rates (hr ⁻¹)	Simulated Monthly Heating and Cooling Load at ELA Air Change Rates (MMBtu)	Estimated Air Exchange Rates with Third floor (hr ⁻¹)
Jan	54.20	0.46	55.26	1.49	95.87	1.03
Feb	38.55	0.4	39.86	1.4	69.15	1.00
Mar	15.13	0.2	20.22	1.29	42.52	1.09
Apr	5.33	0.16	14.3	1.15	27.34	0.99
May	1.81	0.12	4.72	0.94	7.19	0.82
Jun*	n/a	n/a	n/a	0.82	18.54	n/a
Jul*	n/a	n/a	n/a	0.75	19.34	n/a
Aug*	n/a	n/a	n/a	0.74	19.94	n/a
Sep*	n/a	n/a	n/a	0.76	8.44	n/a
Oct	16.58	0.4	13.594	1.05	19.8	0.65
Nov	17.72	0.46	27.74	1.34	45.44	0.88
Dec	45.63	0.5	44.12	1.36	67.94	0.86

(*From June to September, the loads shown in the above table are cooling loads; the measured cooling data is not available; from September to May, the loads shown in the above table are heating loads. There is no overlap between heating and cooling.)



Figure 12. Potential Leakage Sites - Where Ducts Penetrate the Third Floor Ceiling

CONCLUSIONS

Blower door measurements were made in a radiantly heated and cooled office space on Oct. 6 and 10 2006. This paper determines the effective leakage area based on the blower door measurements and estimates year-round infiltration levels in the space, considering the temperature differences and wind speeds. These results give monthly average infiltration rates from 0.74ACH in the summer to 1.49ACH in the winter.

This paper also examines the results of previous infiltration studies of the space that used the tracer gas method, re-analyzes the CO₂ concentration data, and evaluates the infiltration by using logged humidity data. These results for the space infiltration range from 0.78-1.31ACH for the tracer gas method, 0.1-0.9ACH by the CO₂ concentration method, and 0.5-2.5ACH from the logged humidity data, for periods of two to three days.

A significant amount of leaking air has been found to come from the plenum between the space and the third floor below the space. A simulation study of the studied office using DOE2.1 identified an estimated rate of outside air leakage, based on a calibration of the simulation to measured heating consumption data. Combining the results of the calibrated DOE2.1 simulation and the blower door measurement, the third floor air leakage into the space can be estimated. This process gives outside air leakage ranging from 0.1-0.5ACH, while the third floor air leaking into the space appears to range from 0.46-1.09ACH for the periods analyzed.

ACKNOWLEDGEMENTS

This work has been supported by the U.S. Department of Energy via a subcontract with Carnegie Mellon University. The authors want to express their appreciation for the generous assistance of Nina Baird and Fred Betz.

NOMENCLATURE

\dot{m}_{in}	CO ₂ flow into the space, lb/hr
\dot{m}_{out}	CO ₂ flow out of the space, lb/hr
\dot{m}_{gen}	CO ₂ generation in the space lb/hr
V_r	space volume
α	air change rate per hour
ρ	density of CO ₂
A_L	equivalent or effective air leakage area, in ²
Q_r	predicted or measured air flow rate at ΔP_r
ρ	air density, lb _m /ft ³
ΔP_r	reference pressure difference, inches. of water
C_D	discharge coefficient, 0.65
C_5	unit conversion factor, 0.186
\dot{W}_{in}	moisture entering the space by infiltration and mechanical ventilation
\dot{W}_{out}	moisture leaving the space by exhaust air and exfiltration
\dot{W}_{gen}	moisture generated by the occupants
$\dot{W}_{storage}$	moisture storage in the space, assumed to be 0 in this analysis
w_s	mechanical ventilation air humidity ratio, lb/lbda
w_o	outside air humidity ratio, lb/lbda
w_r	indoor humidity ratio, lb/lbda
\dot{V}_s	supply air flow rate, CFM
V_r	space volume, 86000 ft ³
\dot{V}_L	exhaust air and return air flow rate, CFM
α	infiltration rate
ρ	air density lb/ft ³

REFERENCES

- [1] Feustel, H.E., and A. Rayner-Hoosen. 1990. COMIS Fundamentals, LBL-28560. Applied Science Division, Lawrence Berkeley National Laboratory, Berkeley, CA.
- [2] Feustel, H.E. 1999. COMIS-An International multizone air-flow and contaminant transport model. Energy and Buildings, Vol 18. 3-18.
- [3] Sherman, M.H. and D.T. Grimsrud. 1980. Infiltration-pressure correlation:

- Simplified physical modeling. ASHRAE Transactions 86(2), 778-803.
- [4] Walker, I.S. and D.J. Wilson. 1993. Evaluating models for superposition of wind and stack effects in air infiltration. Building and Environment 28(2): 201-210, Pergamon Press.
- [5] Persily, A.K. 1986. Measurement of air infiltration and airtightness in passive solar homes. In Measured air leakage of buildings, P 46. ASTM STP 904. H.R. Trechsel and P.L. Lagus, eds.
- [6] Walker, I.S. and D.J. Wilson. 1998. Field validation of equations for stack and wind driven air infiltration calculations. International Journal of HVAC&R Research 4(2).
- [7] Gong, Xiangyang and David E. Claridge. 2006. Indoor Humidity analysis of an Integrated Radiant Cooling and Desiccant Ventilation System, Proceedings of International Conference for Enhanced Building Operation, Part 1, I-6-1, Nov 6-9, 2006, Shen Zhen, China.
- [8] Mahdavi, A., R. Ries, D. Cho. 2000. Infiltration, Natural Ventilation, and HVAC Performance in the IW, ASHRAE Transactions, 106(1), pp. 728-736.
- [9] Boonyakiat, J. 2003. A model-based approach to ventilation control in buildings, PhD dissertation, Department of Architecture, Carnegie Mellon University.
- [10] Betz, Fred, Z. Bornik, B. Dong, P. Kwok. 2006. CO₂, Occupancy, and Ventilation in an Open-Plan Environment, Project Report, Department of Architecture, Carnegie Mellon University.
- [11] Environment Protection Agency. 2006. Atmosphere changes, accessed in December, 2006, <http://www.epa.gov/climatechange/science/recentac.html>.
- [12] Sherman, Max H, and Darryl J. Dickerhoff. 1998. Airtightness of U.S. Dwellings, ASHRAE Transaction, 104(1), P1359-1367.
- [13] ASHRAE. 2005. ASHRAE Handbook-Fundamentals. Atlanta: American Society of Heating, Refrigeration and Air-Conditioning Engineers, Inc.
- [14] Claridge, David E., N. Bensouda, S.U. Lee, G. Wei, K. Heinemeier, M. Liu. 2003. Manual of Procedures for Calibrating Simulations of Building Systems, Lawrence Berkley National Laboratory, October, 2003.

The indoor CO₂ level can be calculated as follows. CO₂ mass balance in the space can be expressed as the following equation:

$$\frac{dm_{CO_2}}{dt} = \dot{m}_{in} - \dot{m}_{out} + \dot{m}_{gen} \quad (1)$$

where,

$\frac{dm_{CO_2}}{dt}$: indoor CO₂ change with time

Let C_r : indoor CO₂ concentration, PPM

C_o : outdoor CO₂ concentration, PPM,

$$m_{CO_2} = C_r * V_r * \rho * 10^{-6} \quad (2)$$

$$\dot{m}_{in} = C_o * \rho * \alpha * V_r * 10^{-6} \quad (3)$$

$$\dot{m}_{out} = C_r * \rho * \alpha * V_r * 10^{-6} \quad (4)$$

By substituting equations (2), (3), (4) into equation (1), the following equation is obtained:

$$\frac{dC_r}{dt} = -\alpha * \left(C_r - C_o - \frac{\dot{m}_{gen}}{\alpha * V_r * \rho * 10^{-6}} \right) \quad (5)$$

By assuming the initial indoor CO₂ concentration is C_{r0} ppm, the above equation can be solved as

$$C_r = C_o + \frac{\dot{m}_{gen}}{\alpha * V_r * \rho * 10^{-6}} + \left(C_{r0} - C_o - \frac{\dot{m}_{gen}}{\alpha * V_r * \rho * 10^{-6}} \right) e^{-\alpha t} \quad (6)$$

C_r , in the above equation, is the CO₂ level in the space.

APPENDIX 1. DERIVATION OF INDOOR CO₂ CONCENTRATION DECAY MODEL